Requirement for kinase-induced conformational change in eukaryotic initiation factor 2α (eIF2α) restricts phosphorylation of Ser51

Madhusudan Dey[a,b], Algirdas Velyvis[c,d], John J. Li[d,e], Elaine Chiu[d,e], David Chiovitti[d,e], Lewis E. Kay[c,d], Frank Sicheri[d,e,1], and Thomas E. Dever[a,1]

[a]Laboratory of Gene Regulation and Development, Eunice Kennedy Shriver National Institute of Child Health and Human Development, National Institutes of Health, Bethesda, MD 20892; [b]Department of Biological Sciences, University of Wisconsin–Milwaukee, Milwaukee, WI 53211; [c]Departments of Biochemistry and Chemistry, University of Toronto, Toronto, Ontario, Canada M5S 1A8; [d]Department of Molecular Genetics, University of Toronto, Toronto, Ontario, Canada M5S 1A8; and [e]Program in Systems Biology, Samuel Lunenfeld Research Institute, Mount Sinai Hospital, 600 University Avenue, Toronto, Ontario, Canada M5G 1X5

Edited by John Kuriyan, University of California, Berkeley, CA, and approved January 7, 2011 (received for review October 6, 2010)

As phosphorylation of eukaryotic translation initiation factor 2α (eIF2α) on Ser51 inhibits protein synthesis, cells restrict this phosphorylation to the antiviral protein kinase PKR and related eIF2α kinases. In the crystal structure of the PKR–eIF2α complex, the C-terminal lobe of the kinase contacts eIF2α on a face remote from Ser51, leaving Ser51 ∼20 Å from the kinase active site. PKR mutations that cripple the eIF2α-binding site impair phosphorylation; here, we identify mutations in eIF2α that restore Ser51 phosphorylation by PKR with a crippled substrate-binding site. These eIF2α mutations either disrupt a hydrophobic network that restricts the position of Ser51 or alter a linkage between the PKR-docking region and the Ser51 loop. We propose that the protected state of Ser51 in free eIF2α prevents promiscuous phosphorylation and the attendant translational regulation by heterologous kinases, whereas docking of eIF2α on PKR induces a conformational change that regulates the degree of Ser51 exposure and thus restricts phosphorylation to the proper kinases.

The fidelity of signal transduction networks is dependent on both efficient phosphorylation of substrate proteins by the appropriate kinase and prevention of phosphorylation by heterologous kinases. A variety of mechanisms have been adopted to ensure kinase specificity including recognition of flanking residues around the phosphorylation site, kinase-substrate interactions remote from the site of phosphorylation, and the use of scaffolding or adaptor proteins that tether a kinase and its substrate (1). In contrast to protein kinase Cα (PKCα), which phosphorylates a peptide substrate with nearly the same efficiency as an intact folded substrate (2), the K_m for protein kinase PKR phosphorylation of a eukaryotic initiation factor 2α (eIF2α) peptide centered on the key regulatory site Ser51 is roughly 1,000-fold higher than the K_m for intact eIF2α (3, 4). This can be attributed to PKR recognition of the globular fold of eIF2α at a site remote from Ser51 (5). Interestingly, PKC readily phosphorylates the eIF2α peptide, but it is ineffective for phosphorylation of intact eIF2α (the rate is ∼600-fold slower than for the peptide substrate) (3). The inability of PKC to phosphorylate eIF2α is consistent with the notion that eIF2α phosphorylation is restricted to PKR and the family of eIF2α kinases to ensure tight control over the inhibition of protein synthesis caused by eIF2α phosphorylation. However, the precise explanation for why PKC is unable to phosphorylate the Ser51 epitope in intact eIF2α is not resolved.

Phosphorylation of eIF2α is a key regulatory step in protein synthesis. Phosphorylation on Ser51 converts eIF2 from a substrate to an inhibitor of its guanine nucleotide exchange factor eIF2B, and thereby inhibits protein synthesis (reviewed in ref. 6). The eIF2α kinase family consists of four well-conserved members: general control nonderepressible 2 (GCN2), activated by amino acid starvation; PKR, activated by double-stranded RNA and viral infection; PKR-like endoplasmic reticulum kinase (PERK), activated by ER stress; and heme-regulated inhibitor (HRI), activated by low heme levels (reviewed in ref. 7).

The X-ray crystal structure of the PKR kinase domain bound to eIF2α revealed a typical kinase domain architecture consisting of a small N-terminal lobe involved in regulated dimerization and a large C-terminal lobe that engages the eIF2α substrate (5). The N-terminal half of eIF2α, which is sufficient for phosphorylation by the eIF2α kinases (8, 9), contains an oligonucleotide/oligosaccharide-binding (OB)-fold domain composed of five β strands with the Ser51 phosphorylation site located in a conformationally variable loop between strands β3 and β4. In the structure of free yeast eIF2α (10), the Ser51 residue is hidden within a folded configuration flanked by two 3_{10}-helices [$3_{10}A$ (residues 46–50) and $3_{10}B$ (residues 58–61), Fig. 1*A*]. In this conformation, Ser51 would be inaccessible to an attacking protein kinase. In other eIF2α structures, the Ser51 loop is totally disordered. This includes the structure of free human eIF2α^{3-182} (11) and yeast eIF2α^{3-175} in complex with the kinase domain of PKR (5). Likewise, in the solution structure of human eIF2α^{1-304} this same loop displayed greater structural heterogeneity than the rest of the OB-fold domain (12).

As revealed in the structure of the PKR–eIF2α complex, the primary contacts between the two proteins locate to helix αG in the C-terminal lobe of the kinase domain and to a solvent-exposed surface on eIF2α composed by strands β2, β3, and β5, directly opposite to the position of Ser51 in ordered structures (Fig. 1; see also Fig. S7*A*). Notably, helix αG in PKR and other eIF2α kinases is one turn longer and rotated ∼40° relative to its position in other protein kinases (5). As mutations in PKR helix αG impaired eIF2α phosphorylation, but not the ability of PKR to autophosphorylate or phosphorylate a nonspecific substrate like histones (4), helix αG appears to be specifically required for eIF2α recognition and phosphorylation.

Docking the structure of free yeast eIF2α, in which the position of Ser51 is fully resolved, into the PKR-eIF2α cocrystal structure placed Ser51 ∼20 Å from the catalytic base Asp414 of PKR (5). Thus, a significant repositioning of Ser51 from its ordered state is required for it to access the active site of PKR. Whether this is

Author contributions: M.D., A.V., J.J.L., L.E.K., F.S., and T.E.D. designed research; M.D., A.V., and J.J.L. performed research; E.C. and D.C. contributed new reagents/analytic tools; M.D., A.V., J.J.L., L.E.K., F.S., and T.E.D. analyzed data; and M.D., A.V., J.J.L., L.E.K., F.S., and T.E.D. wrote the paper.

The authors declare no conflict of interest.

This article is a PNAS Direct Submission.

[1]To whom correspondence may be addressed. E-mail: sicheri@lunenfeld.ca or tdever@nih.gov.

This article contains supporting information online at www.pnas.org/lookup/suppl/doi:10.1073/pnas.1014872108/-/DCSupplemental.

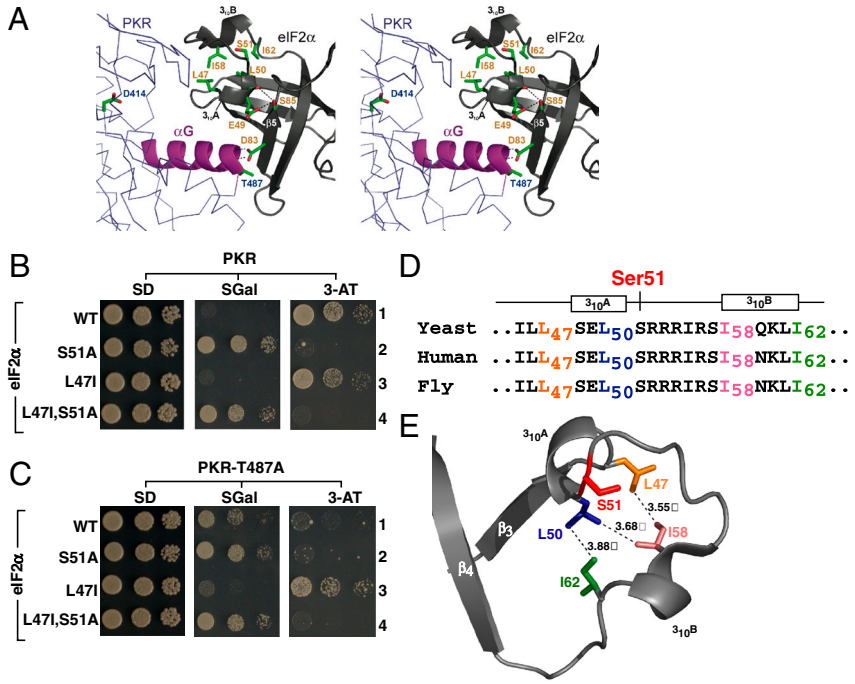

Fig. 1. eIF2α mutation L47I restores PKR–T487A growth phenotypes in yeast. (*A*) Stereo view generated by superposition of the isolated yeast eIF2α structure [Protein Data Bank (PDB) code 1Q46] with the eIF2α–PKR complex (PDB code 2A1A) using PyMOL software (15). Highlighted on the backbone representation of the PKR catalytic domain is helix αG (magenta) with key residue Thr487 and residue Asp414 (active site catalytic base). For clarity, only key eIF2α residues near Ser51 (Glu49 and the hydrophobic network residues Leu47, Leu50, Ile58, and Ile62) and in strand β5 (Asp83 and Ser85) are depicted in stick representation, and the polar contacts involving these residues are shown by dotted lines. (*B* and *C*) eIF2α–L47I mutation enhances PKR–T487A toxicity in yeast. Plasmids expressing PKR (*B*) or PKR–T487A (*C*) under control of a yeast *GAL–CYC1* hybrid promoter were introduced into derivatives of yeast strain H2507 expressing the indicated eIF2α proteins. Transformants were grown to saturation, serially diluted (OD_{600} = 1.0, 0.1, 0.01), and spotted on minimal SD, SGal, and SD supplemented with 3-AT (20 mM) medium and incubated 3 d at 30 °C. (*D*) Conservation of eIF2α sequences flanking Ser51 in *Saccharomyces cerevisiae* (yeast), *Homo sapiens* (human), and *Drosophila melanogaster* (fruit fly). (*E*) The position of Ser51 in free yeast eIF2α (PDB code 1Q46) is restricted by the hydrophobic network consisting of residues L47, L50, I58, and I62.

accomplished simply by the intrinsic conformational flexibility of the Ser51 loop in eIF2α or whether this represents a regulated event remains an open question. Based on the results in this report, we propose that restricted mobility of Ser51 in free eIF2α prevents promiscuous phosphorylation and the attendant translational regulation by heterologous kinases, whereas binding of PKR helix αG to the OB-fold domain of eIF2α triggers a conformational change of the polypeptide region encompassing Ser51 to enable Ser51 to access the PKR active site.

Results

Restoration of PKR-T487A Toxicity in Yeast by an eIF2α–L47I Mutation. Yeast cells lacking the sole endogenous eIF2α kinase GCN2 are unable to grow on medium containing 3-aminotriazole (3-AT), an inhibitor of histidine biosynthesis. Whereas high-level expression of human PKR from a galactose-inducible promoter inhibits yeast cell growth on synthetic galactose (SGal) medium (Fig. 1*B*, *Center*, row 1; and Fig. S1, scheme I), leaky expression of PKR on glucose medium complements the 3-AT–sensitive phenotype (Fig. 1*B*, *Right*, row 1). These growth properties are due to eIF2α phosphorylation as they are suppressed in strains expressing non-phosphorylatable eIF2α–S51A (Fig. 1*B*, row 2). Consistently, immunoblot analysis revealed high levels of Ser51 phosphorylation in cells expressing WT PKR (Fig. 2*A*, lane 1). Substitution of Thr487 in PKR helix αG by Ala or Asp impaired Ser51 phosphorylation (Fig. 2*A*, lane 3) and diminished both the growth inhibitory properties of PKR on SGal medium (Fig. 1*C*, *Center*, row 1; and Fig. S1, scheme II) and the 3-AT–resistant phenotype on synthetic dextrose (SD) medium (Fig. 1*C*, *Right*, row 1).

Using a genetic screen, a single eIF2α mutant (L47I) was found to restore PKR–T487A toxicity in yeast (Fig. 1*C*, *Center*, compare rows 1 and 3; and Fig. S1, scheme III). Random mutagenesis of the Leu47 codon revealed that Val and Cys, like Ile, restored PKR–T487A toxicity (Fig. S2*A*). The L47I mutation also restored growth on 3-AT medium (Fig. 1*C*, *Right*, row 3). These growth properties associated with the eIF2α–L47I mutation were dependent on PKR expression and on phosphorylation of Ser51; note that the phenotypes were suppressed in yeast expressing the double mutant eIF2α–L47I,S51A (Fig. 1*C*, row 4). As expected, the L47I mutation had no impact in cells expressing WT PKR (Fig. 1*B*, rows 1 and 3). Interestingly, the eIF2α–L47I mutation likewise suppressed the 3-AT–sensitive phenotype in cells expressing the GCN2 helix αG mutant T924A (Fig. S2*B*). As the eIF2α–L47I mutation did not confer a 3-AT–resistant phenotype or growth defect in cells lacking an eIF2α kinase (Fig. S2*B*, row 5), the mutation does not function by decreasing eIF2 abundance or by making eIF2 a better inhibitor of eIF2B in the presence or absence of Ser51 phosphorylation. Thus, the L47I mutation in eIF2α compensates for a defective helix αG interaction in either PKR or GCN2 and restores translational regulation.

Disruption of an eIF2α Hydrophobic Network Restores Ser51 Phosphorylation by PKR Helix αG Mutants. The residues flanking the Ser51 phosphorylation site in eIF2α are highly conserved (Fig. 1*D* and Fig. S3), and the position of the Ser51 loop (located between strands β3 and β4 and comprising residues 47–64) in the X-ray structure of free yeast eIF2α (10) is restricted by a hydrophobic network formed by conserved residues L47, L50, I58, and I62 (Fig. 1*E*). Given that the Ser51 loop has been observed in both ordered and disordered states, we reasoned that the hydrophobic interactions might limit the mobility of the loop and provide a means for controlling Ser51 exposure and phosphorylation.

We hypothesized that disruption of the eIF2α hydrophobic network would enhance the mobility of the Ser51 loop and bypass the requirement for the OB-fold–helix αG interaction. To test this idea, we introduced the following single amino acid substitutions into eIF2α: Leu50 by Ser, and Ile58 or Ile62 by Gly. All three eIF2α mutants supported WT growth rates when introduced as the sole copy of eIF2α in yeast (Fig. 2*A*, *Top*, SD medium where PKR is not expressed). High-level expression of WT PKR, but neither PKR–T487D nor the catalytically dead mutant PKR–K296R, resulted in substantial Ser51 phosphorylation and growth inhibition in yeast expressing WT eIF2α (Fig. 2*A*, lanes 1–3). Disruption of the hydrophobic pocket in the eIF2α–L50S, –I58G, and –I62G mutants restored Ser51 phosphorylation by the PKR–T487D mutant (Fig. 2*A*, *Bottom*, lanes 4–6; and Fig. S4). Despite the elevated Ser51 phosphorylation, yeast cell growth was not inhibited in these cells (Fig. 2*A*, SGal panel, lanes 4–6), consistent with the previous finding that this region of eIF2α is critical for the inhibition of eIF2B by phosphorylated eIF2 (8).

The enhanced phosphorylation of the eIF2α mutants in vivo could result from increased Ser51 exposure or from protection from eIF2α phosphatases. To directly examine Ser51 phosphorylation, we performed in vitro kinase assays using [γ-^{33}P]ATP

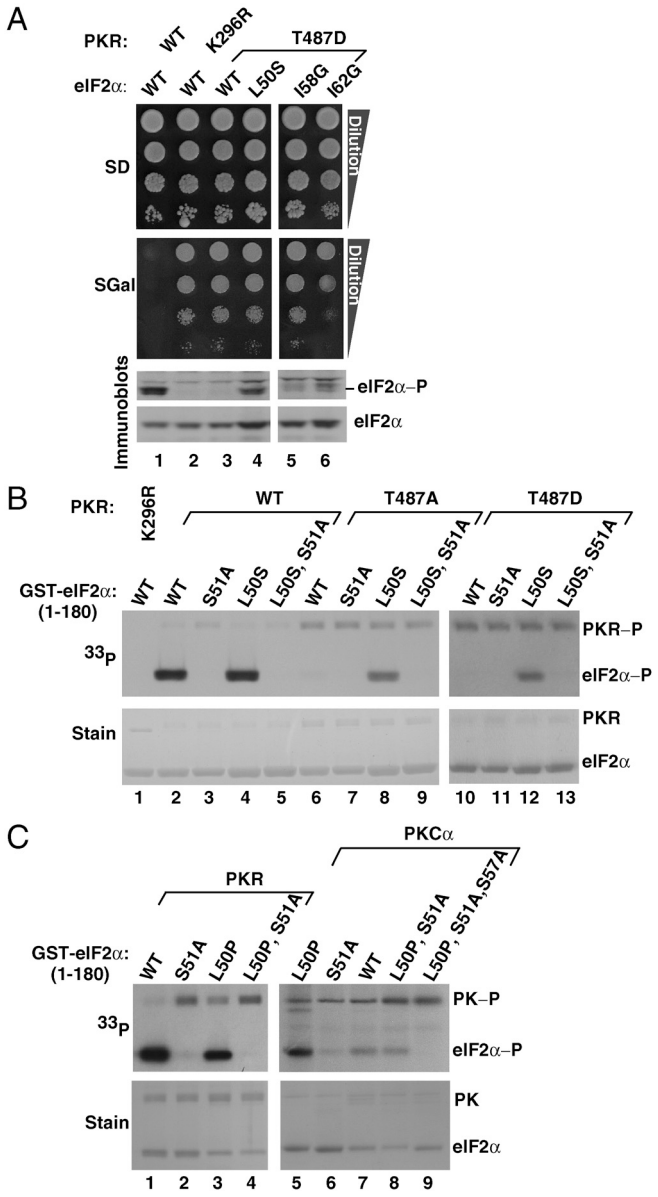

Fig. 2. Disruption of eIF2α hydrophobic network enables Ser51 phosphorylation by PKR helix αG mutants and by PKCα in vitro. (*A*) PKR–T487D phosphorylates Ser51 of eIF2α–L50S, –I58G, and –I62G mutants in vivo. Plasmids expressing WT or mutant versions of eIF2α and PKR, as indicated, were introduced into yeast strain H2507. Transformants were grown, serially diluted, and spotted on SD and SGal medium as described in Fig. 1. WCEs were prepared and subjected to immunoblot analysis to detect eIF2α Ser51 phosphorylation (*Top*) and total eIF2α (*Bottom*). (*B*) eIF2α–L50S mutation restores Ser51 phosphorylation by PKR–T487A and PKR–T487D mutants in vitro. WT PKR or the indicated mutants were purified from yeast and mixed with [γ-^{33}P]ATP and recombinant WT GST–eIF2α^{1-180} or the indicated mutants. Reaction mixtures were resolved by SDS-PAGE, stained with Coomassie blue (*Lower*), and subjected to autoradiography to visualize phosphorylated PKR and eIF2α (PKR-P and eIF2α-P, *Upper*). (C) PKR and PKCα phosphorylate Ser51 of eIF2α–L50P in vitro. GST–eIF2α^{1-180} and its indicated derivatives were mixed with [γ-^{33}P]ATP and either purified PKR or recombinant human PKCα (Invitrogen). Reaction products were analyzed as described in *B*; PK, protein kinase.

and purified WT or mutant forms of PKR and GST–eIF2α^{1-180}. As shown in Fig. 2*B*, WT PKR (lane 2), but not PKR–K296R (lane 1), PKR–T487A (lane 6), or PKR–T487D (lane 10), phosphorylated WT eIF2α. As observed in vivo, the L50S mutation restored eIF2α phosphorylation by PKR–T487A and PKR–T487D (Fig. 2*B*, lanes 8 and 12). Confirming that the L50S mutant substrate was phosphorylated on Ser51, purified GST–eIF2α^{1-180}–L50S,S51A, was not phosphorylated (Fig. 2*B*, lanes 5, 9, and 13). Thus, rather than blocking Ser51 dephosphorylation, disruption of the eIF2α hydrophobic pocket by the L50S mutation enables Ser51 phosphorylation and bypasses the requirement for the eIF2α–PKR helix αG interaction.

Substitution of Pro for Leu50 is expected to not only disrupt the hydrophobic pocket, but also break the $3_{10}A$ helix and shift Ser51 to a more exposed state (Fig. 1*A*). Consistent with this notion, GST–eIF2α^{1-180}–L50P, like the L50S mutant, was phosphorylated in vitro by WT PKR (Fig. 2*C*, lanes 1–4), and the L50P mutation enabled Ser51 phosphorylation by a heterologous kinase. Whereas PKCα poorly phosphorylated GST–eIF2α^{1-180} (Fig. 2*C*, lane 7), PKCα was clearly able to phosphorylate GST–eIF2α^{1-180}–L50P, albeit less efficiently than WT PKR (Fig. 2*C*, lanes 5 and 1). Not all of the PKCα phosphorylation was blocked by the S51A mutation, suggesting that the L50P mutation made other hydroxyl bearing sites in the Ser51 loop accessible to PKCα (Fig. 2*C*, lane 8). Consistent with this idea, mutating both Ser51 and Ser57 to Ala in eIF2α^{1-180}–L50P blocked phosphorylation to below background levels (Fig. 2*C*, lane 9). Taken together, these data indicate that the hydrophobic network in eIF2α restricts the position of Ser51 and prevents promiscuous phosphorylation of Ser51, and other sites in the Ser51 loop, by heterologous kinases and by PKR in the absence of a productive contact between helix αG and the OB-fold domain of eIF2α.

eIF2α–L50S Bypass Mutation Enhances the Mobility of the Ser51 Loop Residues. To assess the impact of the mutations on the eIF2α structure at atomic level, we performed NMR analyses. An overlay of ^{1}H–^{15}N HSQC spectra of WT, L50S, and I62G forms of eIF2α^{1-175} is shown in Fig. 3*A*. The locations of most peaks change little, if at all, as a result of the mutations. Chemical shift differences between backbone amides of the WT eIF2α and either eIF2α–L50S or eIF2α–I62G are restricted to the region around Ser51 and in the regions around residues 30 and 85 (Fig. S5). In particular, residues in the C-terminal helical part of these proteins (residue 100 and beyond) are not perturbed. These results are consistent with all three proteins adopting similar folded structures. The structural perturbation around residues 30 and 85 are consistent with the known structure of eIF2α: These areas pack against the Ser51 loop.

To gain further insight into the relative flexibility of the eIF2α proteins, we used backbone chemical shift measurements to predict the backbone H–N order parameter squared, S^2, for each residue in eIF2α^{1-175} and the respective L50S and I62G mutants using a random coil index (RCI) method (13, 14). S^2 values report on the amplitude of the motion of the amide bond vector with 0 (isotropic motion) $\leq S^2 \leq$ 1 (rigid). As shown in Fig. 3 *B* and *C*, most residues have S^2 values in the 0.8–0.9 range, indicating a small degree of rotational freedom. However, in WT eIF2α^{1-175}, residues 52–57 show greater flexibility, indicating inherent mobility in this region of the protein (Fig. 3*B*). In spectra of the eIF2α^{1-175}–L50S and eIF2α^{1-175}–I62G mutants, chemical shifts of backbone atoms from residues in the Ser51 loop change from ordered-like to much more random coil-like (Ser51 itself is an excellent example of this trend, Fig. 3*C*). Thus, the higher mobility region is both enhanced (lower predicted S^2 values) and broadened to include more residues (Fig. 3*C*) in the two mutants. Taken together, these structural analyses indicate that the hydrophobic network mutations do not affect the overall fold of eIF2α, but instead specifically enhance the mobility of the Ser51 loop.

PKR Enhances Protease Sensitivity of Ser51 Loop in eIF2α. Having observed that the L50S and I62G mutations enhance both Ser51 phosphorylation and the mobility of the Ser51 loop, we hypothesized that binding of PKR would induce a conformational change

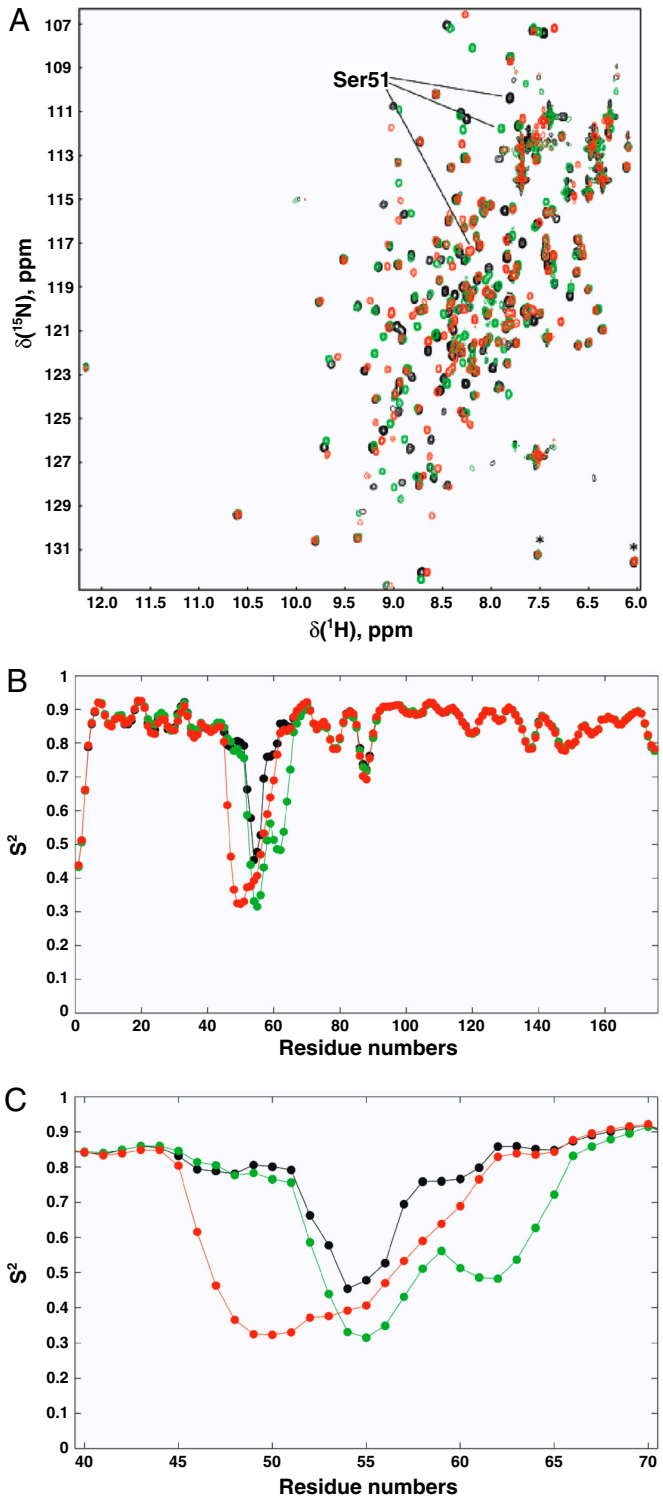

Fig. 3. L50S and I62G mutations enhance mobility of the Ser51 loop in eIF2α. (*A*) Overlay of ^{1}H-^{15}N HSQC spectra of WT–eIF2α^{1-175} (black), and I62G (green) and L50S (red) mutants. Spectra were acquired in 1 h on a 500-MHz spectrometer (room temperature probe head) at 25 °C as described in *SI Methods*. Star denotes folded resonances of Thr128 and Ser161. (*B* and *C*) RCI—predicted order parameters in WT eIF2α^{1-175} (black), eIF2α–I62G$^{1-175}$ (green), and eIF2α–L50S$^{1-175}$ (red). *C* is an enlargement of residues Glu40—Ala70.

in eIF2α and enhance the accessibility of the Ser51 loop to protease digestion. Free yeast eIF2α^{3-175} was susceptible to cleavage by trypsin and thermolysin (Fig. S6*A*) yielding a short ~6 kDa N-terminal fragment and a larger C-terminal fragment starting at Leu61, consistent with the idea that the Ser51 loop samples both protected and exposed states in free eIF2α. Use of dilute concentrations of thermolysin resulted in modest levels of eIF2α cleavage with the majority of the protein remaining intact under the conditions of the limited proteolysis experiment (Fig. 4*A*, lanes 1 and 2; and Fig. S6*B*). Addition of increasing amounts of functional GST–PKR dimers resulted in a corresponding increase in eIF2α cleavage (Fig. 4*A*, lanes 5, 8, and 11). Importantly, this enhanced eIF2α^{3-175} proteolysis was dependent on using functional GST–PKR kinase domain dimers, as addition of inactive PKR kinase domain monomers failed to stimulate the protease sensitivity of eIF2α (Fig. S6*C*). As all assays contained the kinase inhibitor nonhydrolyzable AMPPNP in place of ATP, the increased eIF2α proteolysis was not due to Ser51 phosphorylation. Interestingly, the T487D mutation in helix αG blocked the ability of GST–PKR to enhance eIF2α cleavage (Fig. 4*B*, lane 14 versus 8). Taken together, these data provide direct evidence that PKR induces a conformational change in eIF2α, resulting in increased exposure of the Ser51 loop.

H-Bonding Interactions Involving the $3_{10}A$ Helix Are also Critical for Maintaining Ser51 in a Protected State. PKR helix αG contacts the OB-fold domain of eIF2α on strand β5, which in turn interacts with the $3_{10}A$ helix preceding Ser51. Specifically, the side chain of Ser85 in strand β5 is in position to directly or indirectly (through Arg87 and Arg88) interact with both the backbone carbonyl and the side chain of Glu49 in helix $3_{10}A$ (Fig. 1*A*). We reasoned that these interactions might be important for maintaining Ser51 in a protected state and would provide a physical link between the eIF2α–PKR helix αG contact surface and the conformational state of the Ser51 loop. If correct, disruption of these Ser85 contacts should lead to exposure of Ser51 and bypass the requirement for PKR helix αG docking on the eIF2α OB-fold domain. As predicted, the eIF2α–S85D mutation restored Ser51 phosphorylation by PKR–T487D in vivo (Fig. 5*A*, compare lanes 6 and 3). Likewise, the S85D mutation restored Ser51 phosphorylation in an eIF2α–D83A mutant that perturbs the contact surface with PKR helix αG (Fig. 5*B*, lane 5 versus lane 3). Moreover,

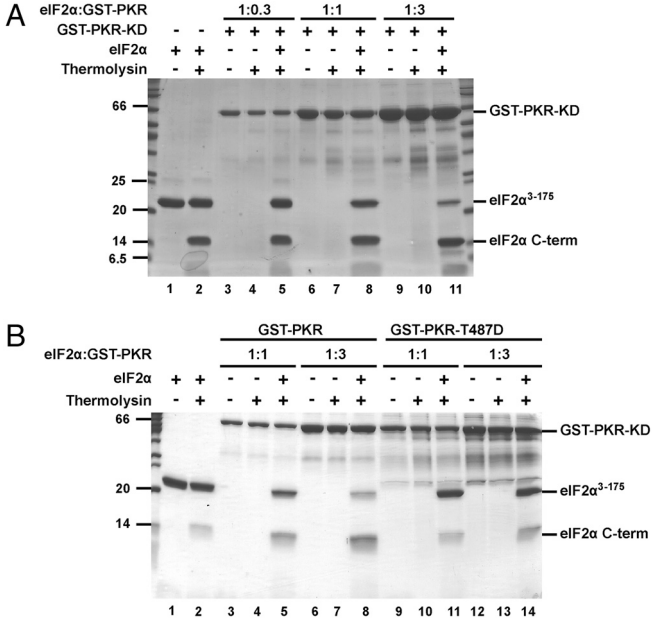

Fig. 4. Addition of PKR enhances protease sensitivity of the Ser51 loop in eIF2α. (*A* and *B*) Purified yeast eIF2α^{3-175} was incubated with thermolysin and the indicated ratio (wt/wt) of purified GST–PKR kinase domain (KD) or mutant GST–PKR–KD–T487D. Protease reaction products were separated by SDS-PAGE and visualized by Coomassie Blue staining. The positions of intact GST–PKR–KD and eIF2α^{3-175}, as well as the eIF2α C-terminal cleavage product (starting at Leu61), are indicated.

the eIF2α–D83A,S85D double mutant was phosphorylated, albeit weakly, by PKR–T487D in vivo (Fig. 5*B*, lane 8). Thus, exposure of Ser51 due to disruption of Ser85 contacts in the eIF2α–D83A,S85D mutant enables Ser51 phosphorylation despite perturbation of the helix αG–OB-fold interaction.

eIF2α–L50S Mutation Enhances Catalytic Efficiency of eIF2α Phosphorylation. Lying at ground zero of the PKR–eIF2α contact site, the side chain of Asp83 in eIF2α strand β5 forms H bonds to the backbone amides of Ala488 and Phe489 at the end of PKR helix αG (Fig. 1 and Fig. S7*A*). In addition, the side chains of Tyr32 in eIF2α strand β2, Met44 in eIF2α strand β3, and Phe489 in PKR helix αG associate through hydrophobic interactions

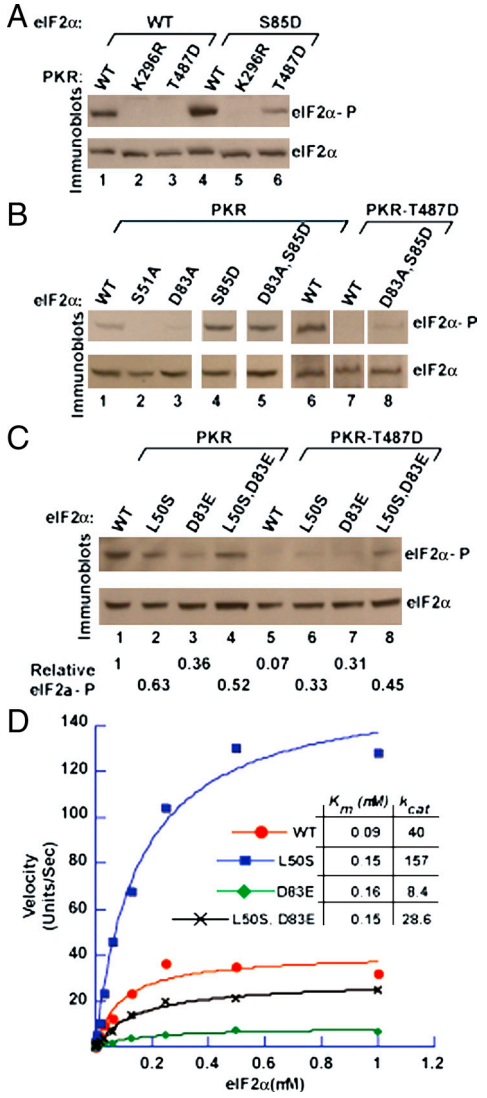

Fig. 5. Mutation of eIF2α at Asp83 or the hydrophobic network residue Leu50 alters the efficiency of Ser51 phosphorylation by PKR. (*A–C*) eIF2α mutations restore Ser51 phosphorylation by PKR–T487D in vivo. WCEs were prepared from strains expressing the indicated WT and mutant forms of eIF2α and PKR and then subjected to immunoblot analysis to detect Ser51-phosphorylated eIF2α (*Upper*) and total eIF2α (*Lower*). In *C* (*Lower*) the relative level of eIF2α phosphorylation in comparison with the strain expressing WT eIF2α and PKR was determined by quantitative densitometry. Results are representative of two independent experiments. (*D*) Kinetic analysis of PKR phosphorylation of eIF2α, eIF2α–D83E, eIF2α–L50S, and eIF2α–L50S, D83E. Phosphorylation of His_6–$eIF2\alpha^{1-200}$ and the indicated mutants by purified PKR was quantified using a PhosphorImager. Results are expressed in arbitrary units and are representative of at least two independent experiments; k_{cat} units are sec^{-1}.

(Fig. S7*A*). Any substitution for Asp83 either impaired (Glu) or abolished (the other 18 amino acids) Ser51 phosphorylation in vivo, and the eIF2α–D83E mutation primarily impaired the k_{cat} for phosphorylation (8) (Fig. 5*D*). Likewise, the eIF2α–M44V mutation had a greater impact on catalysis than on eIF2α binding to PKR (k_{cat} versus K_m effect; Fig. S7*B*). As shown in Fig. 5*C*, the eIF2α–D83E mutation severely impaired Ser51 phosphorylation (lanes 3 and 7 versus 1 and 5, respectively), and phosphorylation of Ser51 in eIF2α–D83E by both WT PKR and PKR–T487D was recovered by the L50S mutation (lanes 4 and 8). The D83E mutation resulted in an ∼80% decrease in the k_{cat} but less than a 2-fold increase in the K_m for phosphorylation by WT PKR (Fig. 5*D*). The L50S mutation partially restored Ser51 phosphorylation in eIF2α–L50S,D83E, increasing the k_{cat} 3-fold with no change in the K_m (Fig. 5*D*, black versus green curves). Consistent with the notion that exposure of Ser51 is a rate-limiting step in the phosphorylation reaction, the L50S mutation increased the k_{cat} for phosphorylation of WT eIF2α by ∼4-fold (Fig. 5*D*, blue versus red curves). Taken together, these data support the notion that following docking of eIF2α on PKR a conformational change is required to expose Ser51 for phosphorylation.

Discussion

Kinase-Induced Conformational Change Exposes Ser51 for Phosphorylation. Our previous structural and mutational analyses on PKR and eIF2α (4, 8) did not reveal how Ser51 gained access to the PKR active site. Docking of the structure of free eIF2α, in which the position of Ser51 is clearly resolved, onto the structure of the PKR–eIF2α complex, placed Ser51 ∼20 Å from the PKR catalytic residue Asp414 (Fig. 1*A*). We considered two models for how Ser51 accessed the phosphoacceptor-binding site in PKR. In the first model, PKR takes advantage of the natural mobility of the eIF2α Ser51 loop. Accordingly, following docking of the eIF2α OB-fold domain onto PKR helix αG, the Ser51 loop spontaneously samples closed and extended conformations. In the extended conformation, Ser51 docks in the kinase active site. Consistent with this model, the Ser51 loop was either not visible or showed signs of structural heterogeneity in X-ray or NMR studies of human or yeast eIF2α (10–12). Our NMR measurements also are consistent with some degree of flexibility in this region, as RCI-derived backbone order parameters (Fig. 3 *B* and *C*) have lower values for residues 52–59. At odds with this model, if Ser51 regularly samples accessible positions, why is it that PKC cannot phosphorylate Ser51 in the context of WT eIF2α but can phosphorylate Ser51 in the context of the different bypass mutations?

In the second model for phosphorylation of Ser51, we propose that docking of eIF2α on PKR induces a conformational change, greater than the normal spontaneous breathing of the Ser51 loop, which enables Ser51 to engage the phosphoacceptor-binding site of the kinase. Consistent with this model, we show that the T487A mutation in PKR helix αG, as well as the D83A mutation in the interacting eIF2α strand β5, impairs Ser51 phosphorylation, and that phosphorylation is recovered by mutation of Ser85 or the hydrophobic network residues Leu47, Leu50, Ile58, and Ile62. Moreover, our limited proteolysis experiments (Fig. 4) provide direct evidence that PKR alters the conformation of the Ser51 loop and enhances its accessibility to protease digestion.

Interestingly, the L50S mutation, through destabilization of the infrastructure that maintains Ser51 in a protected state, enhances the catalytic efficiency of Ser51 phosphorylation of both WT eIF2α and the eIF2α–L50S,D83E double mutant. We propose that these changes in catalytic efficiency reflect the need for an induced conformational change to expose Ser51 in WT eIF2α. Accordingly, as depicted in Fig. 1, docking of eIF2α on PKR helix αG may possibly result in movement of eIF2α strand

β5 and in disruption of direct or indirect contacts between Ser85 in eIF2α strand β5 and Glu49, part of the $3_{10}A$ helix ($S_{48}E_{49}L_{50}$) immediately N-terminal to Ser51. We predict that disruption of this contact and unfolding of the $3_{10}A$ helix destabilizes the hydrophobic network that normally restricts the position of Ser51. Finally, disruption of the hydrophobic network allows the Ser51 loop to adopt an open, extended conformation and enables Ser51 to dock in the kinase catalytic site.

Allosteric Control of Ser51 Exposure Restricts eIF2α Phosphorylation and Ensures Tight Control of Translation. Why has the cell adopted such an elaborate mechanism for Ser51 phosphorylation? We propose that the induced conformational change mechanism restricts Ser51 phosphorylation to the family of eIF2α kinases: PKR, GCN2, PERK, and HRI. As phosphorylation of Ser51 regulates both general and gene-specific protein synthesis, promiscuous phosphorylation of eIF2α by heterologous protein kinases would be deleterious to a cell's functioning and survival. Tight control of Ser51 phosphorylation can be achieved both by regulating the activation of the eIF2α kinases and by preventing Ser51 phosphorylation by other cellular kinases. While the side chain of Ser51 in the structure of isolated yeast eIF2α is chemically exposed in a shallow groove (10), it is not accessible for phosphorylation by a protein kinase. Accordingly, eIF2α is a very poor substrate for phosphorylation by PKC (3) (Fig. 2*C*). We propose that the unique position of helix αG in PKR, which is one turn longer and rotated 40° relative to other kinases (5), enables it to act as an effector to induce the conformational change required for Ser51 to access the kinase active site. By requiring an induced conformational change to expose Ser51 for phosphorylation, translational regulation is restricted to the family of eIF2α kinases that are activated under conditions requiring alterations in protein synthesis.

Methods

Plasmids. See Tables S1 and S2.

Yeast Strains. Strains H1643 (*MATa ura3-52 leu2-3 leu2-112 trp1-Δ63 sui2Δ* p[*SUI2,URA3*]<*GCN4-LacZ,TRP1*>*@trp1*) and H2507 (*MATa ura3-52 leu2-3 leu2-112 trp1-Δ63 gcn2Δ sui2Δ* p[*SUI2,URA3*] were used for in vivo analyses. Strains H1894 (*MATa ura3-52 leu2-3 leu2-112 trp1-Δ63 gcn2Δ*) and J223 (*MATa ura3-52 leu2-3 leu2-112 gcn2Δ, SUI2-S51A*) were used to overexpress *Flag-* and *His*$_6$-tagged *GCN2* and *Flag-* and *His*$_6$-tagged *PKR*, respectively.

Mutagenesis and Screening. Two separate randomly mutagenized DNA libraries were generated in *SUI2*(eIF2α), *LEU2* plasmids using error-prone PCR: one for eIF2α residues 1–48 in plasmid pC171, and the other for residues 84–288 in plasmid p1097. Yeast strain H2507 was transformed with a pEMBLyex4-based *TRP1* plasmid pC3153 that expresses *PKR–T487A* under the control of a *GAL–CYC1* hybrid promoter. The resulting strain was then transformed with the mutated DNA libraries. Approximately 4,000 yeast transformants from each library were selected and replica-printed on medium containing 5-fluoroorotic acid (5-FOA) to select for cell that lost the WT *SUI2, URA3* plasmid. The 5-FOA plates were incubated at 30 °C for 2 d and then replica-printed to SGal medium. The eIF2α plasmid was isolated from the cells that failed to grow on SGal medium, and then the plasmid was retested and sequenced.

Mutations around the eIF2α Ser51 phosphorylation site were generated by PCR. The GST–eIF2α (residues 1–180) plasmids were constructed by PCR amplification of the appropriate DNA fragment from WT or mutant eIF2α templates and then by insertion of the fragment between the *Bam*HI and *Xho*I sites of the expression vector pGEX-6P-1 (Amersham Biosciences).

Immunoblot Analysis to Detect Ser51 Phosphorylation. Yeast transformants expressing PKR under the control of *GAL–CYC1* hybrid promoter were grown in SC-ura medium (synthetic minimal medium containing all amino acids and 2% dextrose, lacking uracil) overnight, diluted to fresh medium to $OD_{600} \sim 0.1$, and grown to $OD_{600} \sim 0.6$. Cells were harvested and transferred to SGal-ura (SC-ura, except 10% galactose) medium and incubated for 2 h to induce PKR expression. Yeast transformants containing GCN2 were grown in SC-Ura-His medium overnight to saturation, diluted to fresh medium to $OD_{600} \sim 0.1$, and grown to $OD_{600} \sim 0.6$. Then, 3-AT (30 mM) was added to the medium, and cells were harvested after 1 h. Whole cell extracts (WCEs) were prepared, separated by SDS-PAGE, and subjected to immunoblot analysis using rabbit phospho-specific antibodies against phosphorylated Ser51 of eIF2α (BioSource International) and rabbit polyclonal antiserum against total eIF2α, as described previously (4).

In Vitro Kinase Assay. Flag- and His_6-tagged PKR and GCN2 were purified from derivatives of strains H1894 and J223, respectively, and used for in vitro kinase assays in kinase buffer (20 mM Tris-HCl pH8.0, 50 mM KCl, 25 mM $MgCl_2$, and 1 mM phenylmethylsulfonyl fluoride) as described earlier (4). Recombinant human PKCα (Invitrogen) was used for in vitro kinase assay in kinase reaction buffer without lipid mixtures (20 mM HEPES pH7.4, 10 mM $MgCl_2$, 100 mM $CaCl_2$, 500 mM ATP, and 5 mCi[γ-^{33}P] ATP).

Limited Proteolysis Experiments. In a 60-uL reaction containing 1 μM AMPPNP in place of ATP to block kinase activity, yeast eIF2α^{3-175} (0.2 mg/mL) was incubated with thermolysin at a 1:3500 wt/wt protease to eIF2α ratio for 30 min at 20 °C. The reaction was quenched by adding SDS-PAGE sample buffer and heating to 90 °C for 1 min. Proteolysis products were separated on 18% acrylamide bis-tris denaturing gels and visualized with Coomassie Blue staining. Cleavage sites were identified by transferring peptide products onto a polyvinylidene difluoride membrane for Edman sequencing at the Advanced Protein Technology Centre, Sick Kids Hospital, Toronto, Canada.

ACKNOWLEDGMENTS. We thank members of the Dever, Sicheri, Kay, and Hinnebusch labs for advice and for discussions. This work was supported in part by the Intramural Research Program of the National Institutes of Health, National Institute of Child Health and Human Development (T.E.D.), by grants from the Canadian Cancer Society to F.S. (Grant 19233), and by grants from the Natural Sciences and Engineering Research Council of Canada and from the Canadian Institutes of Health Research to L.E.K.

1. Ubersax JA, Ferrell JE, Jr (2007) Mechanisms of specificity in protein phosphorylation. *Nat Rev Mol Cell Bio* 8:530–541.
2. Verghese GM, et al. (1994) Protein kinase C-mediated phosphorylation and calmodulin binding of recombinant myristoylated alanine-rich C kinase substrate (MARCKS) and MARCKS-related protein. *J Biol Chem* 269:9361–9367.
3. Mellor H, Proud CG (1991) A synthetic peptide substrate for initiation factor-2 kinases. *Biochem Biophys Res Commun* 178:430–437.
4. Dey M, et al. (2005) Mechanistic link between PKR dimerization, autophosphorylation, and eIF2α substrate recognition. *Cell* 122:901–913.
5. Dar AC, Dever TE, Sicheri F (2005) Higher-order substrate recognition of eIF2α by the RNA-dependent protein kinase PKR. *Cell* 122:887–900.
6. Hinnebusch AG (2000) Mechanism and regulation of initiator methionyl-tRNA binding to ribosomes. *Translational Control of Gene Expression*, eds N Sonenberg, JWB Hershey, and MB Mathews (Cold Spring Harbor Laboratory Press, Cold Spring Harbor), pp 185–243.
7. Dever TE, Dar AC, Sicheri F (2007) The eIF2α kinases. *Translational Control in Biology and Medicine*, eds MB Mathews, N Sonenberg, and JWB Hershey (Cold Spring Harbor Laboratory Press, Cold Spring Harbor, NY), pp 319–344.
8. Dey M, et al. (2005) PKR and GCN2 kinases and guanine nucleotide exchange factor eukaryotic translation initiation factor 2B (eIF2B) recognize overlapping surfaces on eIF2α. *Mol Cell Biol* 25:3063–3075.
9. Krishnamoorthy T, Pavitt GD, Zhang F, Dever TE, Hinnebusch AG (2001) Tight binding of the phosphorylated α subunit of initiation factor 2 (eIF2α) to the regulatory subunits of guanine nucleotide exchange factor eIF2B is required for inhibition of translation initiation. *Mol Cell Biol* 21:5018–5030.
10. Dhaliwal S, Hoffman DW (2003) The crystal structure of the N-terminal region of the alpha subunit of translation initiation factor 2 (eIF2α) from *Saccharomyces cerevisiae* provides a view of the loop containing serine 51, the target of the eIF2α-specific kinases. *J Mol Biol* 334:187–195.
11. Nonato MC, Widom J, Clardy J (2002) Crystal structure of the N-terminal segment of human eukaryotic translation initiation factor 2α. *J Biol Chem* 277:17057–17061.
12. Ito T, Marintchev A, Wagner G (2004) Solution structure of human initiation factor eIF2α reveals homology to the elongation factor eEF1B. *Structure* 12:1693–1704.
13. Shen Y, Delaglio F, Cornilescu G, Bax A (2009) TALOS+: A hybrid method for predicting protein backbone torsion angles from NMR chemical shifts. *J Biomol NMR* 44:213–223.
14. Berjanskii MV, Wishart DS (2005) A simple method to predict protein flexibility using secondary chemical shifts. *J Am Chem Soc* 127:14970–14971.
15. DeLano WL (2004) *The PyMol User's Manual* (DeLano Scientific, San Carlos, CA).